THE JOURNAL OF BIOLOGICAL CHEMISTRY Vol. 280, No. 34, Issue of August 26, pp. 30481–30489, 2005
Printed in U.S.A.

Extracellular Matrix Proteoglycans Control the Fate of Bone Marrow Stromal Cells*

Received for publication, January 18, 2005, and in revised form, May 5, 2005
Published, JBC Papers in Press, June 17, 2005, DOI 10.1074/jbc.M500573200

Yanming Bi‡, Christina H. Stuelten§, Tina Kilts‡, Sunil Wadhwa‡, Renato V. Iozzo¶, Pamela G. Robey‡, Xiao-Dong Chen‡‖, and Marian F. Young‡**

From the ‡Craniofacial and Skeletal Diseases Branch, NIDCR and the §Laboratory of Cell Regulation and Carcinogenesis, NCI, National Institutes of Health, Department of Health and Human Services, Bethesda, Maryland 20892 and the ¶Departments of Pathology, Anatomy, and Cell Biology, Jefferson Medical College, Thomas Jefferson University, Philadelphia, Pennsylvania 19107

Extracellular matrix glycoproteins and proteoglycans bind a variety of growth factors and cytokines thereby regulating matrix assembly as well as bone formation. However, little is known about the mechanisms by which extracellular matrix molecules modulate osteogenic stem cells and bone formation. Using mice deficient in two members of the small leucine-rich proteoglycans, biglycan and decorin, we uncovered a role for these two extracellular matrix proteoglycans in modulating bone formation from bone marrow stromal cells. Our studies showed that the absence of the critical transforming growth factor-β (TGF-β)-binding proteoglycans, biglycan and decorin, prevents TGF-β from proper sequestration within the extracellular matrix. The excess TGF-β directly binds to its receptors on bone marrow stromal cells and overactivates its signaling transduction pathway. Overall, the predominant effect of the increased TGF-β signaling in *bgn*/*dcn*-deficient bone marrow stromal cells is a "switch in fate" from growth to apoptosis, leading to decreased numbers of osteoprogenitor cells and subsequently reduced bone formation. Thus, biglycan and decorin appear to be essential for maintaining an appropriate number of mature osteoblasts by modulating the proliferation and survival of bone marrow stromal cells. These findings underscore the importance of the micro-environment in controlling the fate of adult stem cells and reveal a novel cellular and molecular basis for the physiological and pathological control of bone mass.

The extracellular matrix (ECM)[1] provides structural strength to tissues, maintains the shape of organs, and is often involved directly or indirectly in regulating cell proliferation and differentiation (1–3). ECM components modulate the bioactivities of growth factors and cytokines, such as TGF-β, tumor necrosis factor-α, and platelet-derived growth factor, by 1) activating them by proteolytic processing (4, 5), 2) inactivating them by sequestering and preventing binding to their respective receptors (6–9), or 3) directly binding to cytokine receptors, such as the epidermal growth factor receptor (10, 11).

Proteoglycans, which are characterized by a core protein with at least one glycosaminoglycan chain attached, commonly mediate the interactions of ECM components with growth factors and cytokines (12). Small leucine-rich proteoglycans (SLRPs) are some of the major non-collagen components of the ECM (13). The core proteins of the SLRPs consist of leucine-rich repeats flanked by two cysteine-rich clusters. The size of the core proteins (~40 kDa) is relatively small compared with aggrecan and versican (>200 kDa) (1, 10, 14). The SLRP superfamily currently consists of 13 known members that can be divided into 3 distinct subfamilies based on the genomic organization, structure, and similarity of their amino acid sequences (13). SLRPs are involved in skeletal growth (15–17), craniofacial structure (15), dentin formation (18), and collagen fibrillogenesis (17, 19, 20). However, to date, little is known about the precise mechanism through which SLRPs regulate the formation and maintenance of the skeletal system.

Biglycan (Bgn) and decorin (Dcn) are class I type SLRPs that are expressed in various tissues (7, 15, 21), including bones and teeth. Mice with targeted disruption of the *bgn* gene have impaired postnatal bone formation, which leads to the early onset of osteoporosis (16). Although *Dcn*-deficient mice do not show histological or macroscopical changes in bone (17, 20), they do contain collagen fibrils of abnormal size distribution, density, and shape in mineralized tissue (15, 17). Because of the similarity of their primary sequences as well as their overlapping expression patterns in skeletal tissues, it is not surprising that Bgn and Dcn function redundantly and synergistically. Mice deficient in both *bgn* and *dcn* display more severe defects than mice deficient in either *bgn* or *dcn*, in tissues, such as bone and skin, where Bgn and Dcn are coexpressed (17). These results indicate that Bgn and Dcn may share some common functions in bone and skin and compensate, at least in part, for each other when one is deleted. To eliminate the potential compensation, it is, therefore, necessary to use mice deficient in multiple proteoglycans. Our specific approach was to use *bgn*/*dcn*-deficient mice to study the cellular and molecular mechanisms of ECM proteoglycans in regulating osteogenesis.

Bone marrow stromal cells (BMSCs), which contain skeletal stem cells (also known as mesenchymal stem cells), are derived

* The costs of publication of this article were defrayed in part by the payment of page charges. This article must therefore be hereby marked "*advertisement*" in accordance with 18 U.S.C. Section 1734 solely to indicate this fact.

‖ To whom correspondence may be addressed: University of Arkansas, College of Medicine, 4301 West Markam Str., Slot 587, Little Rock, AR 72205-7199. Tel.: 501-868-1503; Fax: 501-686-8148; E-mail: xdchen@uams.edu.

** To whom correspondence may be addressed: Bldg. 30, Rm. 225, NIDCR, National Institutes of Health, 9000 Rockville Pike, MSC 4320, Bethesda, MD 20892. Tel.: 301-496-8860; Fax: 301-402-0824; E-mail: myoung@dir.nidcr.nih.gov.

[1] The abbreviations used are: ECM, extracellular matrix; SLRPs, small leucine-rich proteoglycans; Bgn, biglycan; Dcn, decorin; BMSCs, bone marrow stromal cells; BrdUrd, bromo-2′-deoxyuridine; BMP2, bone morphogenetic protein 2; Cbfa1, core binding protein; DPBS, Dulbecco's phosphate-buffered saline; TUNEL, terminal deoxynucleotidyl transferase-mediated dUTP and nick end labeling; μCT, microcomputed tomography analysis; WT, wild-type; *p*NA, *p*-nitroanilide.

from clonogenic adherent bone marrow cells, which are colony-forming units-fibroblastic. Under certain conditions, BMSCs can give rise to osteoblasts, chondrocytes, adipocytes, myelosupportive stroma, and even muscle and nerve tissue (22–24). These cells have been used for both *in vivo* and *in vitro* studies to understand the mechanisms that modulate skeletal formation and pathological changes in bone disease. *In vivo* xenogenic transplantation of BMSCs mimics bone formation where transplanted BMSCs can form a miniature bone organ that contains bone, adipocytes, and hematopoiesis-supporting stroma. They can form cartilage in micromass cultures *in vitro* (23, 25). BMSCs have also been used to examine the ability of osteogenic stem cells to proliferate, differentiate, and form mineral nodules *in vitro* (25, 26). BMSCs, therefore, permit in-depth analysis of the signal transduction pathways that regulate proliferation, survival, and differentiation of osteogenic stem cells.

In the current studies, we utilized BMSCs from *bgn*/*dcn*-deficient mice to examine the combined effects of Bgn and Dcn on bone formation. We found that BMSCs deficient in both SLRPs have increased TGF-β signaling due to the inability to sequester TGF-β in the ECM by Bgn and Dcn, resulting in switched fate from growth to apoptosis. The premature death of osteogenic stem cells and osteoblast precursors led to a decreased number of mature osteoblasts thereby contributing to decreased osteogenesis and an osteoporosis-like phenotype in *bgn*/*dcn*-deficient mice. Our studies demonstrate, for the first time, an unsuspected role for these two SLRPs in controlling bone mass by regulating TGF-β activity, which in turn modulated the proliferation and survival of osteogenic stem cells. This provides a new paradigm in understanding the molecular basis of osteoporosis caused by low bone formation.

MATERIALS AND METHODS

Animals—All experiments were performed using 8-week-old *WT*, and *bgn*/*dcn*-deficient C3H/HeNHsd male mice under an institutionally approved protocol for the use of animals in research (NIDCR-DIR-03-280). Generation of *bgn*/*dcn*-deficient mice has been previously reported (16, 17, 20). The genotype of the *WT* ($bgn^{+/0}dcn^{+/+}$, *bgn* is on the X but not Y chromosome) and *bgn*/*dcn*-deficient ($bgn^{-/0}dcn^{-/-}$) mice was determined by a PCR-based assay as described previously (16, 17, 20).

Culture Medium and Preparation of BMSCs—The culture medium for BMSCs was α-minimal essential medium (Invitrogen), supplemented with 20% lot-selected fetal bovine serum (BD Biosciences, Franklin Lakes, NJ), 2 mM glutamine, 100 units/ml penicillin, 100 μg/ml streptomycin (BioFluids, Rockville, MD), and 10 nM dexamethasone (Sigma). The osteogenic induction medium was the culture medium supplemented with 100 μM ascorbic acid 2-phosphate (WAKO, Tokyo), and 2 mM β-glycerophosphate (Sigma).

Bone marrow cells ($10–20 \times 10^6$) in culture medium containing 55 μM 2-mercaptoethanol (Invitrogen) were plated into a 100-mm tissue culture dish. The cells were incubated until ~80% confluence (12–14 days) then washed with PBS to remove non-adherent cells. The adherent cells were detached with 200 units/ml collagenase, and plated for the experiments as described below for each assay.

Colony Forming Efficiency—Colony forming efficiency assays were performed as previously described (27, 28). Colonies containing more than 50 cells were counted using a dissecting microscope. Because each colony is theoretically formed from a single stem cell, this permits a direct estimate of the stem cell colony forming efficiency by counting the number of colonies formed by 1×10^6 marrow cells originally plated.

Proliferation of BMSCs—BMSCs (3×10^4/well) were plated into an 8-well chamber slide (Nalge Nunc International, Naperville, IL) and cultured (5% CO_2, 37 °C) overnight. The cells were labeled with bromo-2′-deoxyuridine (BrdUrd) labeling reagent (Zymed Laboratories, South San Francisco, CA) for 24 h and fixed in 70% alcohol for 20 min at 4 °C. The BrdUrd-labeled cells were visualized using the BrdUrd Staining Kit (Zymed Laboratories Inc.) following procedures recommended by the manufacturer.

In Vitro Calcium Accumulation—BMSCs (2×10^5/well) were plated into a 12-well plate and cultured until confluent. Culture medium was then replaced with osteogenic induction medium in the presence or absence of 200 ng/ml bone morphogenetic protein 2 (BMP2) (Wyeth Research, Cambridge, MA). After 6 weeks, calcium deposits were detected by staining with 2% Alizarin Red S (pH 4.2, Sigma). To quantify the stained nodules, the stain was solubilized with 0.5 ml of 5% SDS in 0.5 N HCl for 30 min at room temperature (29). Solubilized stain (0.15 ml) was transferred to wells of a 96-well plate, and absorbance was measured at 405 nm.

In Vivo Bone Formation—Approximately 3×10^6 BMSCs were mixed with 40 mg of hydroxyapatite/tricalcium phosphate ceramic powder (Zimmer Inc., Warsaw, IN) and then transplanted subcutaneously into the dorsal surface of 10-week-old immunocompromised beige mice (NIH-bg-nu-xid, Harlan Sprague-Dawley, Indianapolis, IN) as previously described (30). These procedures were performed in accordance to specifications described in an animal protocol approved by an institutional review board (NIDCR 02-222). The transplants were harvested after 8–9 weeks, fixed in freshly prepared 4% paraformaldehyde at 4 °C for 2–3 days, decalcified with buffered 10% EDTA (pH 8.0) at 4 °C for 1–2 weeks, and then processed for standard paraffin embedding. Three representative H&E-stained histological sections for each transplant were chosen for the quantitation of new bone generated. The percentage of new bone formed in transplants was measured by computer assisted histomorphometry using Scion Image (Scion Corp., Frederick, MD) or ImageJ (NIH Image, rsb.info.nih.gov/nih-image/).

Western Blot Analysis—Confluent BMSCs were treated with 2 ng/ml TGF-β1 (R&D Systems, Minneapolis, MN) or vehicle for 30 min or 48 h. The protein extraction and Western blot analyses were done as previously described (31). The primary antibodies included rabbit anti-Bax, -Bad, -p-Smad2, and -Smad2 (1:500, Cell Signaling, Beverly, MA); rabbit anti-Hsp90 and -TGF-β receptor types I and II (1:500, Santa Cruz Biotechnology, Inc., Santa Cruz, CA); rabbit anti-Smad3 (1:500, Calbiochem); or rabbit anti-Cbfa1 (1:100, Oncogene Research Product, Cambridge, MA).

Northern Blot Analysis—Confluent BMSCs were treated with 200 ng/ml BMP2 or vehicle in osteogenic induction medium for 2 weeks. The total RNA was isolated using RNA STAT-60 Reagent (TEL-TEST "B" Inc., Friendswood, TX) according to the manufacturer's recommendations. Northern blot analyses were performed as previously described (31).

Enzyme-linked Immunosorbent Assay—BMSCs (5×10^4/well) were plated into a 24-well plate and cultured to confluence (5% CO_2, 37 °C). The cells were cultured in α-minimal essential medium media with 3% bovine serum albumin overnight, treated with vehicle or 2 ng/ml TGF-β1 in α-minimal essential medium media containing 0.1% bovine serum albumin for 30 min. The culture medium was collected for measurement of TGF-β concentration. Attached cells were washed twice with PBS and then fixed with freshly prepared 2% paraformaldehyde for 30 min at room temperature for analysis of matrix-bound TGF-β1. Concentrations of TGF-β1 in the culture media were measured using the DuoSet Elisa Development System (R&D Systems). The TGF-β1 binding to cell surface and sequestered in the ECM was detected using a biotin-conjugated TGF-β1-specific antibody (chicken, 36 μg/ml, R&D Systems) after blocking nonspecific binding with Reagent Diluent (R&D Systems). Streptavidin-horseradish peroxidase (R&D Systems) was added for 20 min to bind the immobilized biotinylated anti-TGF-β1 antibody. The substrate (tetramethylbenzidine/hydrogen peroxide, R&D Systems) reacted with horseradish peroxidase to develop color. Color development was stopped with 2 N H_2SO_4, and the intensity of the color was measured at $A_{450\ nm}$ and corrected at $A_{560\ nm}$ using a microplate reader. The amount of TGF-β1 was calculated from a TGF-β1 standard curve and was normalized by protein content. The protein content of attached cells was measured using a BCA Protein Assay Kit (Pierce).

Confocal Fluorescence Microscopy—BMSCs (1×10^5/well) were plated into a 12-well plate containing an 18-mm round coverslip (Fisher, Pittsburgh, PA) and cultured to 70–80% confluence (5% CO_2, 37 °C). The cells were fixed with 2% paraformaldehyde in DPBS (Dulbecco's phosphate-buffered saline) for 20 min at room temperature, washed with 0.1% (w/v) glycine (ICN, Aurora, OH) in DPBS, blocked 1 h at room temperature with 0.5% (w/v) casein (Sigma) in DPBS, and incubated with anti-TGF-β1 antibody (chicken, 1:50, R&D Systems) in blocking buffer overnight at 4 °C, followed by incubation with anti-chicken IgY~fluorescein isothiocyanate antibody in DPBS (1:500, Jackson Laboratories, West Grove, PA) for 1 h at room temperature. Specimens were washed with DPBS and again fixed with 4% paraformaldehyde in DPBS for 10 min at room temperature, and washed with 0.1% glycine in DPBS. Specimens were mounted using 4′,6-diamidino-2-phenylindole containing mounting medium (Vector Laboratories, Burlingame, CA), and immunoreactivity of the specimens was visualized using a Leica DM IRBE confocal microscope and the

supplied software (Leica confocal software version 2.00).

Apoptosis of BMSCs—BMSCs (3×10^4/well) were plated into an 8-well chamber slide and cultured for 2–3 days (5% CO_2, 37 °C). The cells were then treated with vehicle or 1 μM staurosporine (Alexis, San Diego, CA) for 4 h or 2 ng/ml TGF-β1 for 48 h. At indicated time points, the cells were washed twice with PBS and then fixed with freshly prepared 1% paraformaldehyde for 10 min at room temperature. Cells undergoing apoptosis were detected by immunohistochemical staining with a terminal deoxynucleotidyl transferase-mediated dUTP and nick end-labeling (TUNEL) assay using the ApopTag Plus Peroxidase In Situ Apoptosis Detection Kit (Chemicon, Temecula, CA), following procedures recommended by the manufacturer.

Caspase-3 Activity of BMSCs—Confluent BMSCs were treated with vehicle, 2 ng/ml TGF-β1, or 2 ng/ml TGF-β1 plus 3 μM caspase-3 inhibitor (benzyloxycarbonyl-DEVD-fluoromethyl ketone, BioVision, Mountain View, CA) in osteogenic induction medium for 5 or 6 h. The caspase-3 activity of BMSCs was measured using the BD ApoAlert™ Caspase Colorimetric Assay Kit (BD Biosciences) following procedures recommended by the manufacturer except that the caspase-3 activity was normalized by protein content. The protein content of cells was measured using a BCA Protein Assay Kit (Pierce).

Immunohistochemistry—Mouse embryos were removed immediately prior to birth (E19.5), dissected, fixed in cold freshly prepared Millonig's Modified Phosphate Buffered formalin (Surgipath, St. Louis, MO) at 4 °C for 3 days, and then transferred into 70% ethanol. The fixed samples were processed for standard paraffin embedding and sectioning. Enzymatic immunochemistry staining of TGF-β was performed using the broad spectrum immunoperoxidase AEC kit (SuperPicTure™ Polymer Detection Kit, Zymed Laboratories Inc.), following procedures recommended by the manufacturer. The sections were blocked with 10% goat serum (Zymed Laboratories Inc.) and incubated with specific primary antibody recognizing TGF-β1 (mouse, clone 9016, 1:50 in 10% goat serum, R&D Systems) or mouse IgG1 control at the same dilution (R&D Systems) overnight at 4 °C. Apoptotic cells were detected by immunohistochemical staining with a TUNEL assay using the KLE-NOW-FragEL™ DNA Fragmentation Detection Kit (Oncogene, San Diego, CA), following procedures recommended by the manufacturer.

Microcomputed Tomography Analysis—Femurs were scanned and reconstructed with 8-μm isotropic voxels on a μCT system (eXplore MS, GE Medical Systems, London, Ontario, Canada). A bone standard (SB3, Gammex RMI, Middleton, WI) was also scanned using the same protocol and used for the calibration of bone mineral density measurements. The reconstructed three-dimensional imagines of distal femurs were analyzed using MicroView (GE Medical Systems, London, Ontario, Canada). A fixed threshold was used to separate the bone and marrow phase. The trabecular bone mineral density and bone volume per tissue volume in the distal femur were measured in an elliptical cylinder ($1.3 \times 0.6 \times 1.9$ mm) within the metaphysis.

Statistical Analysis—All figures are representative of at least three experiments. All data are presented as mean ± S.E. Statistical analyses were done by using Student's *t* test.

RESULTS

Osteogenesis of BMSCs Is Decreased in the Absence of Bgn and Dcn in Vitro and in Vivo—We have previously shown that *bgn/dcn*-deficient mice exhibit a more severe reduction in bone mass compared with wild-type (*WT*) mice or mice deficient in either *bgn* or *dcn* (17). Microcomputed tomography (μCT) analysis showed that the trabecular bone mineral density and bone volume per tissue volume in the metaphyses of the distal femur of *bgn/dcn*-deficient mice were lower than *WT* mice at 6 weeks of age (Fig. 1). Moreover, the osteopenic phenotype was more profound with aging (Fig. 1). To investigate the cellular mechanism of this severe osteopenia in the absence of both Bgn and Dcn, we hypothesized that the defect in BMSCs could be related to impaired bone formation in *bgn/dcn*-deficient mice. To test this hypothesis, we assessed the ability of osteogenic stem cells to calcify *in vitro* using Alizarin Red S staining that allows visualization of Ca^{2+} accumulation. Ca^{2+} accumulation in *bgn/dcn*-deficient BMSC cultures was much lower than that in *WT* cell cultures (Fig. 2*A*). Because Ca^{2+} accumulation was relatively low in both *WT* and *bgn/dcn*-deficient cultures, we treated the BMSCs with BMP2, a stimulator of osteogenesis (32, 33). BMP2 dramatically increased Ca^{2+} accumulation (Fig. 2*A*, *right*). Quantitation of Alizarin Red S staining showed that Ca^{2+} accumulation in the cultures of BMSCs from *bgn/dcn*-deficient mice was 51.6 ± 4.4% less than that of *WT* cell cultures in the presence or absence of BMP2 (Fig. 2*A*, *right*). These results indicated that the *in vitro* calcification ability of BMSCs was decreased in the absence of Bgn and Dcn.

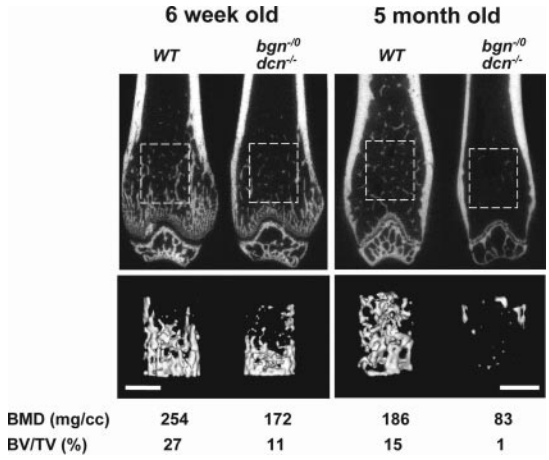

FIG. 1. **Trabecular bone mineral density and volume decreased in mice deficient in both Bgn and Dcn.** The *top panels* are μCT images of the distal femoral metaphyses (*top*) from 6-week-old (*left panels*) and 5-month-old (*right panels*) wild-type (*WT*) and *bgn/dcn*-deficient ($bgn^{-/0}/dcn^{-/-}$) mice. The *bottom panels* show reconstructed three-dimensional images of trabecular bone in a selected elliptical cylinder ($1.3 \times 0.6 \times 1.9$ mm) within the metaphyses (shown above in *dashed boxes*). The trabecular bone mineral density and bone volume per tissue volume in the distal femur were measured in the elliptical cylinder. *Bar*, 1 mm.

To further extend our *in vitro* results, we assessed the ability of BMSCs to form bone *in vivo* using transplantation experiments. In those experiments, BMSCs from *bgn/dcn*-deficient or *WT* mice were mixed with hydroxyapatite/tricalcium phosphate and transplanted subcutaneously into the dorsal subcutis of immunocompromised mice. Although bone tissue was formed from both *bgn/dcn*-deficient and *WT* BMSCs at 8 weeks after transplantation (Fig. 2*B*, *left*), BMSCs from *bgn/dcn*-deficient mice generated 82 ± 4% less bone than the cells from *WT* mice (Fig. 2*B*, *right*). Collectively, both *in vitro* and *in vivo* results suggested that the defect in osteogenesis by BMSCs contributed, at least in part, to the impaired bone formation in *bgn/dcn*-deficient mice. The impaired bone formation in the absence of Bgn and Dcn could be due to a defect in the differentiation of BMSCs. However, the expression levels of core binding protein (Cbfa1/Runx2), an essential regulator of osteoblast differentiation, and the osteoblast marker osteopontin, were not affected by the lack of both proteoglycans (Fig. 2*C*). The expression level of bone sialoprotein in *bgn/dcn* double-deficient BMSCs was higher than in *WT* cells in both the presence or absence of BMP2 (Fig. 2*C*). Those results suggested that the impaired bone formation in the absence of Bgn and Dcn was not due to a decrease in differentiation capacity of BMSCs.

The Number of BMSCs Decreases in the Absence of Bgn and Dcn—Because the differentiation of BMSCs was not decreased in the absence of Bgn and Dcn, we speculated that a decrease in the number of osteogenic stem cells might be the reason for decreased bone formation. To measure this, colony forming efficiency assays were performed to determine the number of BMSCs present in bone marrow. The results showed that there were substantially fewer colonies formed in the cultures derived from *bgn/dcn*-deficient bone marrow compared with the *WT* bone marrow (Fig. 3*A*, *left*). Quantitative evaluations showed that 66 ± 5% fewer colonies were formed in *bgn/dcn*-deficient bone marrow cell

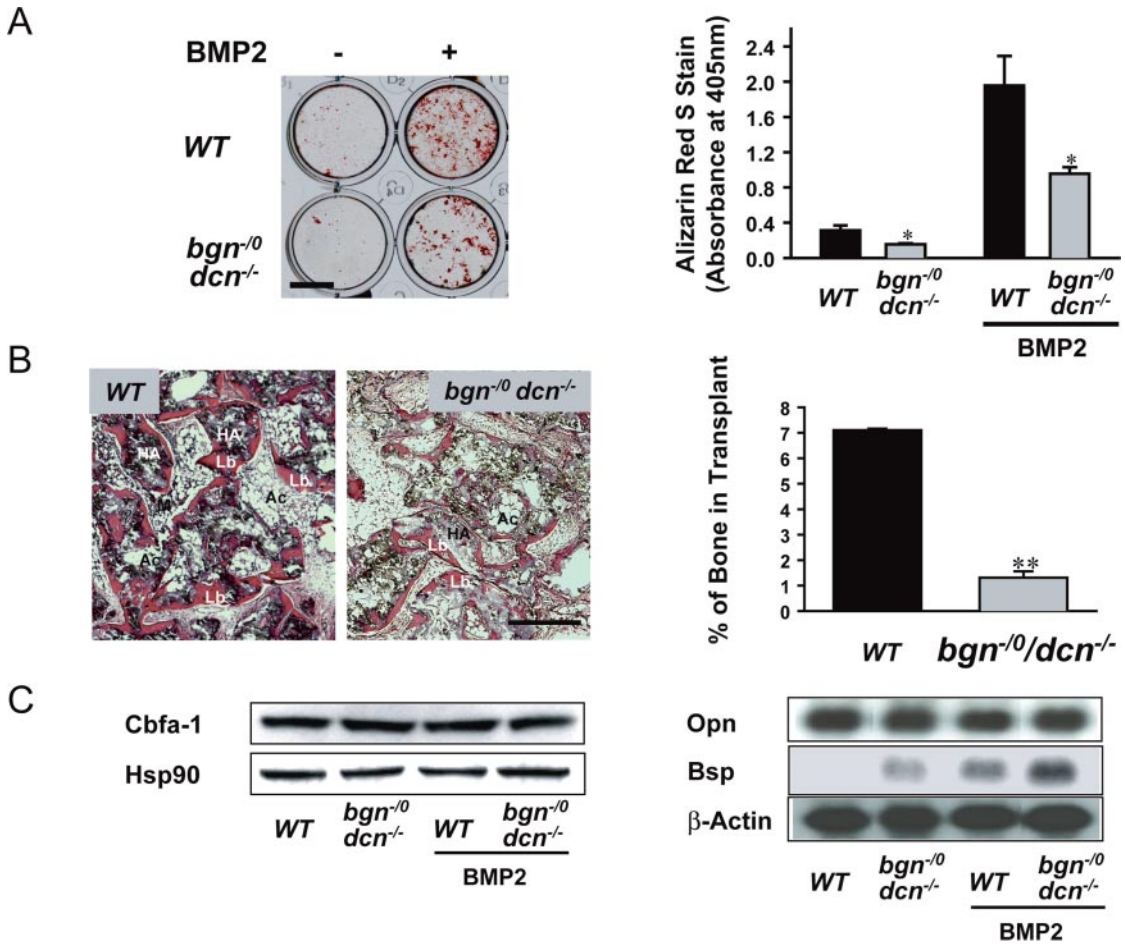

FIG. 2. **The bone formation from BMSCs *in vitro* and *in vivo* decreases in the absence of Bgn and Dcn.** *A*, photographs are the culture wells of Alizarin Red S stained Ca^{2+} deposition after BMSCs from wild-type and *bgn/dcn*-deficient mice were cultured in osteogenic induction medium in the presence (*right wells*) or absence (*left wells*) of BMP2 for 6 weeks. *Bar* = 10 mm. The *graph* on the *right* shows the quantitative evaluation of Alizarin Red S staining. Data are reported as means ± S.E. ($n = 3$). *, denotes $p < 0.05$ compared with *WT* BMSCs. *B*, histological sections are the transplants of *WT* (*left*) and *bgn/dcn*-deficient (*right*) BMSCs after 9 weeks post-transplantation. Lamellar bone (*Lb*) was formed on the HA/TCP surfaces (*HA*). Marrow organ (*M*) with adipocytes (*Ac*) was surrounded by bone. *Bar* = 500 μm. The *graph* on the *right* shows the quantitative results of the percentage of bone formed in the transplant. The results represent the average of three histological sections (50×) from *left*, *middle*, and *right* areas of whole transplant. **, $p < 0.0001$ compared with *WT* BMSCs. *C*, Western blot analysis (*left*) shows the expression of Cbfa1 48 h after BMSCs were cultured in the presence or absence of 200 ng/ml BMP2. Hsp90 expression level was used as a loading control. Northern blot analysis (*right*) shows the expression of osteopontin (*Opn*) and bone sialoprotein (*Bsp*) 2 weeks after BMSCs were cultured in osteogenic induction medium in the presence or absence of 200 ng/ml BMP2. β-Actin expression level was used as a loading control.

cultures compared with *WT* cultures (average of seven independent experiments) (Fig. 3*A*, *right*). This data demonstrated that the number of osteogenic stem cells was significantly decreased in the absence of both Bgn and Dcn.

Apoptosis of BMSCs Increases in the Absence of Bgn and Dcn—Changes in the proliferation or survival of BMSCs could affect the number of osteoprogenitor cells and subsequently alter the number of mature osteoblasts. We, therefore, theorized that a decrease in proliferation and/or survival of BMSCs was responsible for the lower number of BMSCs in *bgn/dcn*-deficient mice. To determine the proliferation rate of BMSCs *in vitro*, we used BrdUrd incorporation assay. As shown in Fig. 3*B*, the number of dividing cells in the *bgn/dcn*-deficient BMSCs was 44.5 ± 7.9% higher than that of *WT* cells after overnight growth (Fig. 3*B*, *left*). This experiment demonstrated that proliferation of BMSCs was increased in the absence of Bgn and Dcn.

Because the decreased number of BMSCs in the absence of Bgn and Dcn is not due to decreased proliferation of BMSCs, we next determined the effect of Bgn and Dcn on the survival of BMSCs *in vitro*. TUNEL staining of BMSCs showed that the number of apoptotic cells in the *bgn/dcn*-deficient BMSC culture was higher compared with the *WT* cell culture (Fig. 3*C*). When BMSCs were treated with a potent apoptotic inducer, staurosporine, the number of apoptotic BMSCs from *bgn/dcn*-deficient mice was still higher compared with *WT* cells (Fig. 3*C*). Therefore, the decrease in the number of osteogenic stem cells in the *bgn/dcn*-deficient mice is due to increased apoptosis rather than decreased proliferation of BMSCs.

Our *in vitro* findings suggested that increased apoptosis of osteogenic stem cells might lead to an insufficient number of mature osteoblasts and decreased bone formation. To confirm this *in vivo*, we examined apoptosis in the endosteum of the growth plates of the legs and ribs. The endosteum that lines the surface of the marrow cavity is composed of thin layers of mesenchymal cells and contains abundant osteoprogenitors at this embryonic stage. TUNEL staining showed that there were substantially more TUNEL-positive cells (*arrows*) in the endosteum (Fig. 4) at the bone collar region of growth plates in *bgn/dcn*-deficient mice (Fig. 4, *c* and *d*) compared with *WT* mice (Fig. 4, *a* and *b*). Increased apoptosis was also found in the bone marrow of *bgn/dcn*-deficient mice compared with *WT* mice (Fig. 4, *e* and *f*). Some of the apoptotic cells were observed on the surface of trabecular bone (*asterisk*, Fig. 4, *g* and *h*). Similarly, in ribs more apoptotic endosteum cells were found in *bgn/dcn*-deficient mice as compared with WT mice (Fig. 4, *i* and *j*). These

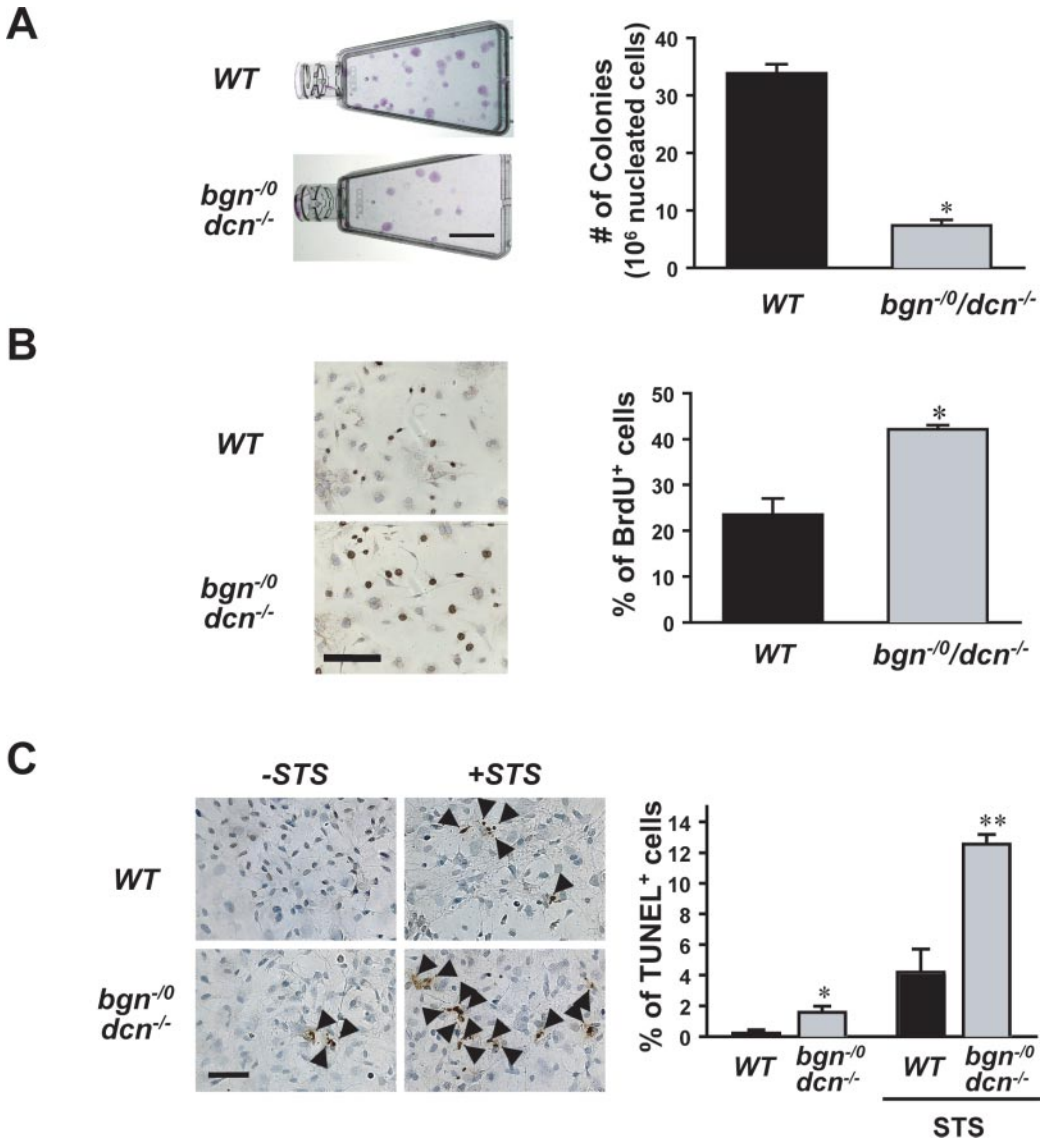

FIG. 3. **Increased apoptosis of BMSCs leads to decreased number of BMSCs in bone marrow in the absence of Bgn and Dcn.** *A*, photographs are the culture flasks showing colonies formed from 1 million *WT* or *bgn/dcn*-deficient bone marrow nucleated cells after 14 days of culture. The colonies were positive for both methyl violet and alkaline phosphatase (data not shown). *Bar* = 20 mm. The *graphs* on the *right* show the number of colonies that were counted using a dissecting microscope. Data are reported as means ± S.E. ($n = 5$). *, $p < 0.0001$ compared with *WT* culture. *B*, the proliferation of BMSCs was measured by overnight BrdUrd labeling. The percentage of BrdUrd-positive cells (*brown*) was quantified by scoring all of the cells in randomly chosen field (×200) on chamber slides of each sample. Data are reported as means ± S.E. ($n = 3$–4). *Bar* = 50 μm. *, $p < 0.007$ compared with *WT* BMSCs. *C*, apoptosis of BMSCs was visualized by TUNEL staining after incubating with or without staurosporine (*STS*, 1 μM) for 4 h. *Bar* = 50 μm. Quantitative evaluation of apoptosis is represented by the percentage of TUNEL-positive cells. Apoptotic cells (*arrows*) were quantified by scoring all of the cells in randomly chosen fields (×400) on a chamber slice of each sample. The results are the average of three fields of each sample. *, $p < 0.04$; **, $p < 0.008$ compared with *WT* BMSCs.

results suggested that there was increased apoptosis in osteoprogenitors and pre-osteoblasts. Thus, our *in vitro* and *in vivo* results demonstrate that the decreased number of cells in the osteoblastic lineage in *bgn/dcn*-deficient mice was due to increased apoptosis of osteoprogenitors.

Sequestration of TGF-β in the ECM Is Disrupted in the Absence of Bgn and Dcn—To understand the underlying mechanisms that cause increased proliferation and apoptosis of BMSCs in the absence of Bgn and Dcn, we focused on the growth factors and cytokines that are regulated by Bgn and Dcn. It has been shown that both Bgn and Dcn bind to TGF-β (7) and regulate its effects on osteoblasts and their precursors (27). It was predicted that Bgn and Dcn would bind TGF-β and sequester it within the ECM. We further speculated that the distribution of TGF-β might be altered in the absence of Bgn and Dcn. Immunohistochemistry of sections of femur with a monoclonal antibody specific for TGF-β1 showed that the immunoreactivity in the regions containing hypertrophic chondrocytes, trabecular bone, and bone marrow of WT mouse femur section was remarkably greater than comparable *bgn/dcn*-deficient tissues (Fig. 5*A*). To quantify the levels of TGF-β, we did an *in vitro* experiment to determine the relative amount of TGF-β1 that binds to the cell layer (cell surface and ECM) in confluent cultures of BMSCs using a biotin-conjugated TGF-β1-specific antibody. Consistent with immunohistochemistry of femoral sections, the amount of TGF-β1 was much higher in the cell layer of WT BMSCs compared with *bgn/dcn*-deficient BMSCs (Fig. 5*B*). These results suggested that the amount of TGF-β sequestered in the ECM was decreased in the absence of Bgn and Dcn. We, therefore, theorized that TGF-β cannot be trapped in the ECM when both Bgn and Dcn are absent, subsequently leaving TGF-β free. To test this concept, we decided to measure the concentration of TGF-β in the media *versus* in the cell layers. However, the basal level of TGF-β in the culture

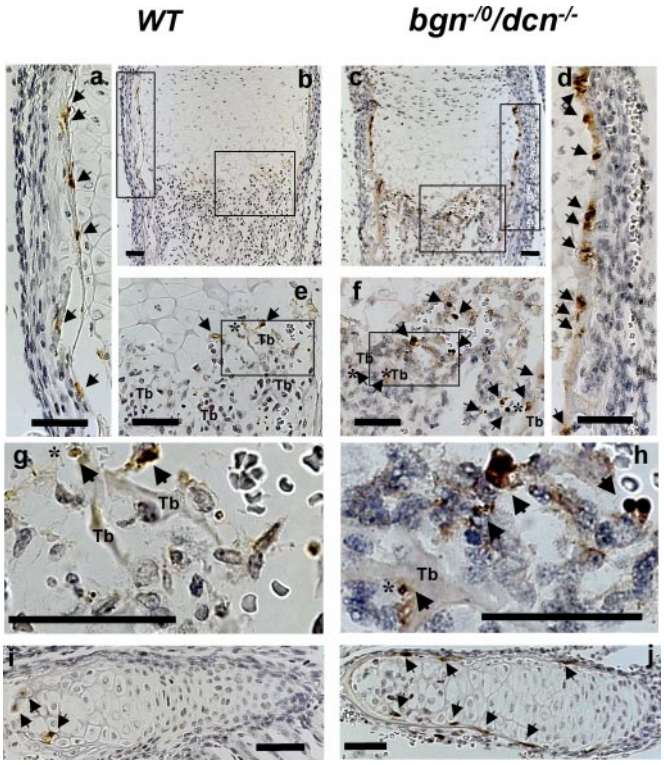

FIG. 4. **Apoptosis of osteoprogenic cells *in vivo* increases in the absence of Bgn and Dcn.** Histological sections show the bone collar regions of *WT* (*b*) and *bgn/dcn*-deficient (*c*) mouse tibia that stained for TUNEL (*brown*) and counterstained with hematoxylin. Higher magnification (×400) of selected *WT* (*a*) endosteum area in *b* and *bgn/dcn*-deficient (*d*) endosteum area in *c* shows apoptotic osteogenic cells (*arrows*). Higher magnification (×400) of selected *WT* (*e*) bone marrow region in *b* and *bgn/dcn*-deficient (*f*) bone marrow region in *c* shows TUNEL-positive cells (*arrows*) in the bone marrow. *g* and *h* are the higher magnifications of selected areas in *e* and *f*, respectively. *, TUNEL-positive cells on the surface of trabecular bone. Histological sections of ribs of *WT* (*i*) and *bgn/dcn*-deficient (*j*) mice stained for TUNEL (*brown*) and counterstained with hematoxylin. *Arrows* on the histological section indicate TUNEL-positive cells. *Bars* = 50 μm.

media was undetectable. We took a different approach, in which we added 2 ng/ml TGF-β1 into the confluent culture of BMSCs and then measured the TGF-β1 that remained in the medium and bound to the cell layer. Fig. 5*C* (*left*) shows that the level of TGF-β1 remaining in the *bgn/dcn*-deficient BMSC culture medium was higher than that in WT culture medium. In contrast, the level of TGF-β1 binding to the cell layer of *bgn/dcn*-deficient BMSCs was lower than that binding to the WT layer (Fig. 5*C*, *right*). Overall, these results supported our hypothesis that Bgn and Dcn sequester TGF-β in the ECM.

BMSCs Are Hyper-responsive to TGF-β in the Absence of Bgn and Dcn—*In vivo* and *in vitro* analysis of the BMSC microenvironment suggested that TGF-β could not be sequestered in the ECM in the absence of Bgn and Dcn and therefore, the excess TGF-β would be free. We, therefore, hypothesized that the free TGF-β would bind to its receptors to activate its signal transduction pathway. To confirm our hypothesis, we examined the amount of TGF-β1 bound to the surface of WT and *bgn/dcn*-deficient BMSCs in the sub-confluent cultures of BMSCs. Confocal microscopic study showed substantially higher levels of active TGF-β1 on the surface of *bgn/dcn*-deficient BMSCs compared with WT cells (Fig. 6*A*). Furthermore, Western blot analysis showed that the expression of TGF-β receptors I and II in *bgn/dcn*-deficient BMSCs was higher than that in *WT* cells (Fig. 6*B*), possibly due to positive regulation by TGF-β1 (34, 35). We therefore predicted that TGF-β signaling would be increased in *bgn/dcn*-deficient BMSCs as compared with WT cells. To test this, we examined the expression of molecules that are critical to the TGF-β signaling transduction. TGF-β binds to its receptors and signals specifically through phosphorylation of members of the Smad family, Smad2/3, which then form heterodimers with Smad4. The heterodimers translocate to the nucleus and act as transcription factors regulating cell growth and survival (36, 37). The expression levels of both Smad2 and Smad3 were higher in *bgn/dcn*-deficient BMSCs compared with *WT* cells in the presence or absence of TGF-β1 (Fig. 6*C*). Smad2 was rapidly phosphorylated in both *WT* and *bgn/dcn*-deficient BMSCs upon treatment with 2 ng/ml TGF-β1 (Fig. 6*C*). However, the expression level of p-Smad2 in *bgn/dcn*-deficient BMSCs was much higher than that in *WT* cells. These data clearly show that TGF-β signaling in BMSCs was increased in cells lacking Bgn and Dcn.

Increased TGF-β Signaling in the Absence of Bgn and Dcn Leads to Increased Apoptosis of BMSCs—Increased TGF-β signaling might alter the functions of TGF-β in regulating BMSCs. When BMSCs were treated with 2 ng/ml TGF-β1, the cells rapidly proliferated (data not shown) and formed condensed nodules in both *WT* and *bgn/dcn*-deficient cultures. However, BMSCs in *bgn/dcn*-deficient cultures detached from tissue culture plates and died after 6 days of treatment with TGF-β1. In contrast, *WT* BMSCs were unaffected (Fig. 7*A*). These results suggest that BMSCs from *bgn/dcn*-deficient mice responded differently to TGF-β1 and underwent premature death.

It has been reported that overexpression of Smad3 in the presence of TGF-β significantly induces apoptosis (38, 39). To test whether the premature death of BMSCs in the absence of Bgn and Dcn was due to increased apoptosis, we examined apoptosis of BMSCs in the presence or absence of TGF-β1. TUNEL staining showed that there were substantially more TUNEL-positive cells in *bgn/dcn*-deficient BMSC cultures (Fig. 6*B*). TGF-β1 up-regulated the expression of Smad-3 (Fig. 6*C*) and accordingly increased apoptosis of BMSCs (Fig. 7*B*). Caspase-3 is a key protease in the execution of apoptosis (40). To examine whether the TGF-β1-induced death of BMSCs was mediated by caspase-3, we added a caspase-3 inhibitor to the TGF-β1-treated BMSC cultures. As expected, the caspase-3 inhibitor did prevent TGF-β1-induced death of BMSCs (Fig. 7*A*).

To understand the molecular mechanisms of the accelerated apoptosis in *bgn/dcn*-deficient BMSCs, we examined the expression of pro-apoptotic Bcl-2 family proteins and the protease activity of caspase-3. Fig. 7 shows that the expression of pro-apoptotic proteins, Bax and Bad, was higher in *bgn/dcn*-deficient BMSCs than that in *WT* cells. The expression of both the active and the truncated form of Bad was slightly higher in *bgn/dcn*-deficient cells compared with WT cells in the presence and absence of TGF-β1 (Fig. 7*C*). TGF-β1 increased the expression of Bax in both *WT* and *bgn/dcn*-deficient cells. However, the expression level of Bax was higher in *bgn/dcn*-deficient BMSCs than in WT cells. The protease activity of caspase-3 was significantly higher in *bgn/dcn*-deficient BMSCs than that in *WT* cells (Fig. 7*D*). TGF-β1 increased the activity of caspase-3 in both *WT* and *bgn/dcn*-deficient BMSCs (Fig. 7*D*). The protease activity of caspase-3 was still significantly higher in *bgn/dcn*-deficient BMSCs (Fig. 7*D*). This partially explains the early onset of TGF-β1-induced death of *bgn/dcn*-deficient BMSCs. Taken together, it appears that the TGF-β1 signaling is increased in the absence of Bgn and Dcn, leading to switch the fate of BMSCs from growth to apoptosis.

DISCUSSION

We have previously shown that *bgn/dcn* double-deficient mice have lower bone mass in trabecular and cortical bones compared with *WT* mice (17). We now could demonstrate that

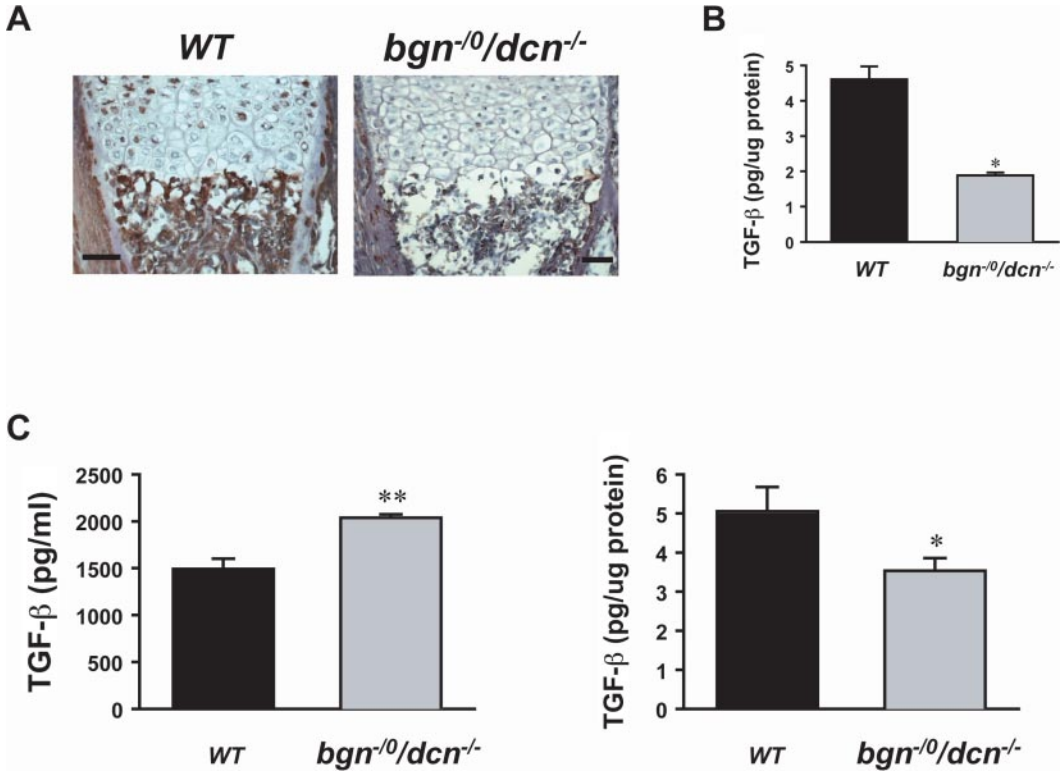

FIG. 5. **The sequestration of TGF-β1 in ECM is disrupted in the absence of Bgn and Dcn.** *A*, representative histological sections of bone collar regions of *WT* (*left*) and *bgn/dcn*-deficient (*right*) mouse tibia were stained with anti-TGF-β1 antibody and counterstained with hematoxylin. *Bars* = 50 μm. *B*, TGF-β1 bound to the cell layer (cell surface and ECM) of confluent BMSC cultures. The levels of TGF-β1 bound to the cell layer were detected by a biotin-conjugated TGF-β1 specific antibody and normalized with protein content. Data are reported as means ± S.E. (n = 3–4). *, $p < 0.001$ compared with *WT* BMSCs. *C*, TGF-β1 remaining in the culture media (*left*) and bound to the cell layer (*right*) after treatment with 2 ng/ml TGF-β1 for 30 min. The concentration of TGF-β1 in the culture media was measured by enzyme-linked immunosorbent assay. Data are reported as means ± S.E. (n = 4–6). *, $p < 0.05$ and **, $p < 0.003$ compared with *WT* BMSCs.

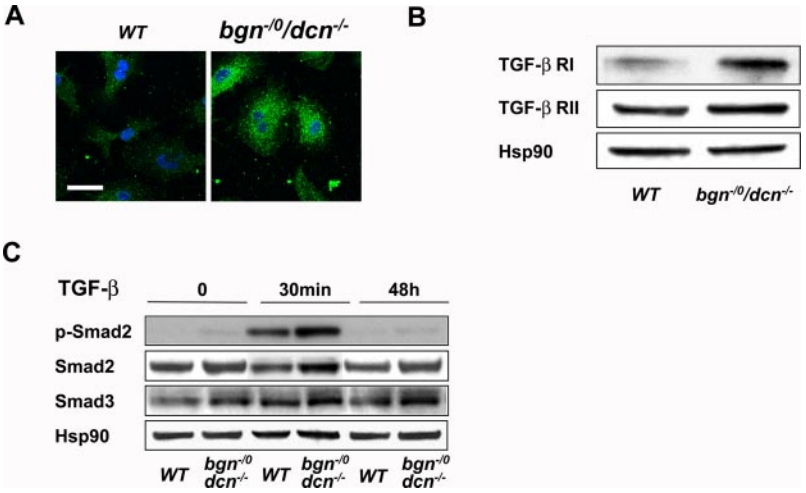

FIG. 6. **TGF-β signaling in BMSCs increases in the absence of Bgn and Dcn.** *A*, confocal microscopy shows an increased level of active TGF-β1 (*green*) on the surface of *bgn/dcn*-deficient BMSCs (*right*) as compared with BMSCs from WT (*left*). Nuclei were stained with 4′,6-diamidino-2-phenylindole (*blue*). *Bar* = 25 μm. *B*, Western blot analysis shows the expression of TGF-β receptors I and II in BMSCs from WT and *bgn/dcn*-deficient mice. *C*, Western blot analysis shows the expression of Smads 30 min and 48 h after BMSCs were treated with 2 ng/ml TGF-β1. Hsp90 expression levels were used as a loading control.

this reduction in bone mass was at least in part due to increased apoptosis of *bgn/dcn*-deficient BMSCs and consequently dramatic reduction in the number of BMSCs. A deeper investigation of the mechanisms showed that the lack of Bgn and Dcn prevents TGF-β from proper sequestration within the ECM, resulting in higher levels of free TGF-β available to bind to its receptors and, consequently, overactivating its signaling through the Smad pathway. Overactivated TGF-β signaling played a central role in promoting apoptosis in the *bgn/dcn*-deficient BMSCs. Our results demonstrate that these two ECM proteoglycans are involved in controlling proliferation and survival of BMSCs and, subsequently, maintaining appropriate numbers of mature osteoblasts by controlling the availability of TGF-β to osteoprogenitors.

TGF-β is abundant in the ECM of bone and regulates proliferation, differentiation, and mineralization of osteoprogenitors and osteoblasts (41–43). Both large and small proteoglycans in the ECM interact with cytokines and growth factors and regulate their function (2, 12, 44). The ECM serves as storage for TGF-β and controls its activity (43). TGF-β is a well studied growth factor in terms of binding to proteoglycans, such as betaglycan, Bgn, Dcn, and fibromodulin (7, 45). *In vivo* administration of Dcn prevents fibrosis caused by overexpression of TGF-β in human and experimental animal models (46–48). *In vitro*, Dcn inhibits the binding of TGF-β to macrophages, and in turn reverses the TGF-β-induced proliferation and adhesion of macrophages (49). Overexpression of Bgn or Dcn could neutralize TGF-β-induced cell growth, collagen gel retraction, and

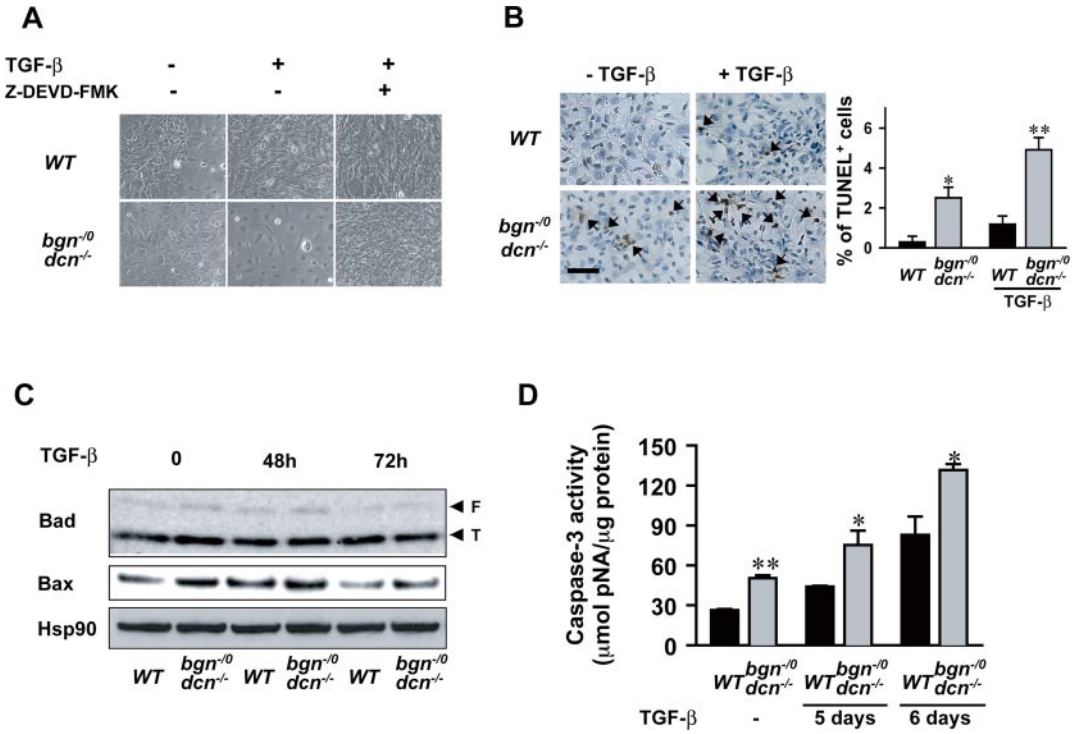

FIG. 7. **The expression of pro-apoptotic proteins in BMSCs increases in the absence of Bgn and Dcn.** *A*, phase contrast light microscopy (×200) shows the post-confluent BMSCs cultures after treatment with vehicle, 2 ng/ml TGF-β1, or 2 ng/ml TGF-β1 plus 3 μM caspase-3 inhibitor benzyloxycarbonyl-DEVD-fluoromethyl ketone (*Z-DEVD-FMK*)) in osteogenic induction medium for 6 days. *B*, apoptosis of BMSCs was measured by TUNEL staining after treatment with vehicle or 2 ng/ml TGF-β1 for 48 h. *Bar* = 50 μm. Apoptotic cells were quantified by scoring all of the cells in three randomly chosen fields (×400) on a chamber slide of each sample. Data are reported as means ± S.E. ($n = 3$). *, $p < 0.03$ and **, $p < 0.007$ compared with the percentage of TUNEL-positive *WT* BMSCs. *C*, Western blotting analysis shows the expression of pro-apoptotic proteins, truncated (*T*) Bad, full-length (*F*) Bad and Bax 48 and 72 h after BMSCs were treated with 2 ng/ml TGF-β1. Hsp90 expression level was used as a loading control. *D*, the protease activity of caspase-3 was measured by the detection of the chromophore *p*-nitroanaline (*pNA*) after *p*NA was cleaved by caspase-3 from *p*NA-labeled caspase-3-specific substrate. The units of caspase-3 activity were quantified using a standard curve of free *p*NA. The protease activity of caspase-3 was normalized with protein content. Data are reported as means ± S.E. ($n = 3$). *, $p < 0.05$ and **, $p < 0.0005$ compared with the caspase-3 activity of *WT* BMSCs at the same time point.

expression of matrix protein (6, 50, 51). However, the TGF-β-mediated stimulation of collagen gel retraction and expression of Bgn is not affected by adding free Dcn to the culture medium (51), suggesting that Dcn controls TGF-β biological activity by sequestering it into the ECM. Nevertheless, those studies have not shown evidence that Bgn and Dcn sequester TGF-β in the ECM to regulate its activity. Here, we present for the first time direct evidence that Bgn and Dcn modulate TGF-β biological activity by sequestering it in the ECM. Similarly, BMP2, another member of the TGF-β superfamily, might also be regulated by Bgn and Dcn with the same mechanism. The expression of its signaling components, Smad1 and phosphorylated Smad1, were higher in *bgn/dcn*-deficient BMSCs compared with *WT* cells (data not shown), which could also explain the higher expression of bone sialoprotein (Fig. 2*C*).

We clearly demonstrate that TGF-β signaling in BMSCs increases in the absence of both Bgn and Dcn due to loss of the sequestration of TGF-β in the ECM. Dysfunction of TGF-β activation has been found in other pathological conditions (52, 53). TGF-β is an important regulator of osteogenesis (43, 54). Although the induction of TGF-β signaling in the absence of Bgn and Dcn is modest, the impact of this modest induction on tissues could be very significant, because it is constitutive. Increased TGF-β signaling could be the major mechanism that causes the osteopenic phenotype in the *bgn/dcn*-deficient mice. Consistent with our findings, a similar phenotype is observed in the transgenic mice that overexpress TGF-β2 in osteoblasts via an osteocalcin promoter-driven transgene (55). Furthermore, inhibition of TGF-β signaling by expressing the dominant-negative form of TGF-β II receptor in transgenic mice causes a high bone mass phenotype (55, 56). Therefore, alteration of the TGF-β signaling could affect bone mass.

TGF-β regulates cell growth, differentiation, and apoptosis in a variety of cells (57–60). It has been reported that increased activation of TGF-β promotes apoptosis in different tissues (52, 53, 61). TGF-β stimulates proliferation of osteoprogenitor cells and ECM formation, but inhibits differentiation and mineralization of mature osteoblasts (41–43, 62). Our studies revealed multiple roles for TGF-β in the regulation of BMSCs during osteogenesis. TGF-β stimulated proliferation of BMSCs and subsequently induced apoptosis. The switch in the fate of BMSCs from growth to programmed cell death depends on the activity, concentration, and duration of TGF-β treatment. The "TGF-β Hyperactive" BMSCs in the absence of Bgn and Dcn proliferated faster and underwent apoptosis prematurely. It has been shown in other cell culture systems that the biological effects of TGF-β could change under different circumstances, which can result in switching the fate of cells from one dominant activity to the other (59, 63). For example, Hagedorn *et al.* (63) reported that the concentration of TGF-β controls the fate of neural progenitor clusters between neurogenesis and apoptosis. The majority of neural progenitor clusters choose neuronal fate at lower concentrations of TGF-β, but apoptosis at higher concentrations. Not only TGF-β, but also another member of the TGF-β superfamily, BMP2, favored neural differentiation at lower concentrations and apoptosis at higher concentrations (64). Apoptosis is a necessary process during development and maintenance of homeostasis in adult tissues (65). TGF-β controls the appropriate numbers of mature osteoblasts through its dual effects on proliferation and apoptosis of

osteogenic stem cells during skeletal development and bone remodeling (66, 67). Alteration of TGF-β activity could interrupt the balance between growth and death. The induction of premature death in osteogenic stem cells by an overactivated TGF-β signaling pathway would then lead to insufficiency of mature osteoblasts in *bgn/dcn*-deficient mice, causing a decrease in osteogenesis.

In summary, we show for the first time that ECM proteoglycans control the fate of bone marrow stromal cells. Our findings are important for several reasons. First, knowing the functions of ECM proteoglycans in regulating osteogenesis is critical for understanding how the skeleton is developed and, specifically, how the integrity of skeleton is maintained, and for understanding age-related skeletal diseases, such as osteoporosis. Second, our results reveal the importance of micro-environment in developing and maintaining the skeletal system. Third, our findings on the regulation of osteogenic stem cells by ECM proteoglycans provide a new target for developing therapeutic approaches for osteoporosis.

Acknowledgments—We are grateful to Drs. Michael T. Collins, Larry W. Fisher, Kathleen C. Flanders, Edward M. Greenfield, Anita B. Roberts, Songtao Shi, and Li Zhang for many helpful discussions.

REFERENCES

1. Hocking, A. M., Shinomura, T., and McQuillan, D. J. (1998) *Matrix Biol.* **17,** 1–19
2. Kresse, H., and Schonherr, E. (2001) *J. Cell. Physiol.* **189,** 266–274
3. Iozzo, R. V. (1997) *Crit. Rev. Biochem. Mol. Biol.* **32,** 141–174
4. Munger, J. S., Harpel, J. G., Gleizes, P. E., Mazzieri, R., Nunes, I., and Rifkin, D. B. (1997) *Kidney Int.* **51,** 1376–1382
5. Gleizes, P. E., Munger, J. S., Nunes, I., Harpel, J. G., Mazzieri, R., Noguera, I., and Rifkin, D. B. (1997) *Stem. Cells* **15,** 190–197
6. Hausser, H., Groning, A., Hasilik, A., Schonherr, E., and Kresse, H. (1994) *FEBS Lett.* **353,** 243–245
7. Hildebrand, A., Romaris, M., Rasmussen, L. M., Heinegard, D., Twardzik, D. R., Border, W. A., and Ruoslahti, E. (1994) *Biochem. J.* **302,** 527–534
8. Nili, N., Cheema, A. N., Giordano, F. J., Barolet, A. W., Babaei, S., Hickey, R., Eskandarian, M. R., Smeets, M., Butany, J., Pasterkamp, G., and Strauss, B. H. (2003) *Am. J. Pathol.* **163,** 869–878
9. Tufvesson, E., and Westergren-Thorsson, G. (2002) *FEBS Lett.* **530,** 124–128
10. Iozzo, R. V., Moscatello, D. K., McQuillan, D. J., and Eichstetter, I. (1999) *J. Biol. Chem.* **274,** 4489–4492
11. Santra, M., Reed, C. C., and Iozzo, R. V. (2002) *J. Biol. Chem.* **277,** 35671–35681
12. Schonherr, E., and Hausser, H. J. (2000) *Dev. Immunol.* **7,** 89–101
13. Iozzo, R. V., and Murdoch, A. D. (1996) *FASEB J.* **10,** 598–614
14. Hardingham, T. E., and Fosang, A. J. (1992) *FASEB J.* **6,** 861–870
15. Ameye, L., and Young, M. F. (2002) *Glycobiology* **12,** 107R–116R
16. Xu, T., Bianco, P., Fisher, L. W., Longenecker, G., Smith, E., Goldstein, S., Bonadio, J., Boskey, A., Heegaard, A. M., Sommer, B., Satomura, K., Dominguez, P., Zhao, C., Kulkarni, A. B., Robey, P. G., and Young, M. F. (1998) *Nat. Genet.* **20,** 78–82
17. Corsi, A., Xu, T., Chen, X. D., Boyde, A., Liang, J., Mankani, M., Sommer, B., Iozzo, R. V., Eichstetter, I., Robey, P. G., Bianco, P., and Young, M. F. (2002) *J. Bone Miner Res.* **17,** 1180–1189
18. Goldberg, M., Septier, D., Rapoport, O., Young, M., and Ameye, L. (2002) *J. Dent. Res.* **81,** 520–524
19. Ameye, L., Aria, D., Jepsen, K., Oldberg, A., Xu, T., and Young, M. F. (2002) *FASEB J.* **16,** 673–680
20. Danielson, K. G., Baribault, H., Holmes, D. F., Graham, H., Kadler, K. E., and Iozzo, R. V. (1997) *J. Cell Biol.* **136,** 729–743
21. Bianco, P., Fisher, L. W., Young, M. F., Termine, J. D., and Robey, P. G. (1990) *J. Histochem. Cytochem.* **38,** 1549–1563
22. Pittenger, M. F., Mackay, A. M., Beck, S. C., Jaiswal, R. K., Douglas, R., Mosca, J. D., Moorman, M. A., Simonetti, D. W., Craig, S., and Marshak, D. R. (1999) *Science* **284,** 143–147
23. Bianco, P., Riminucci, M., Gronthos, S., and Robey, P. G. (2001) *Stem. Cells* **19,** 180–192
24. Owen, M. (1988) *J. Cell Sci. Suppl.* **10,** 63–76
25. Friedenstein, A. J., Piatetzky, S., II, and Petrakova, K. V. (1966) *J. Embryol. Exp. Morphol.* **16,** 381–390
26. Bianco, P., and Robey, P. G. (2001) *Nature* **414,** 118–121
27. Chen, X. D., Shi, S., Xu, T., Robey, P. G., and Young, M. F. (2002) *J. Bone Miner Res.* **17,** 331–340
28. Kuznetsov, S., and Gehron Robey, P. (1996) *Calcif. Tissue Int.* **59,** 265–270
29. Kostenuik, P. J., Halloran, B. P., Morey-Holton, E. R., and Bikle, D. D. (1997) *Am. J. Physiol.* **273,** E1133–E1139
30. Krebsbach, P. H., Kuznetsov, S. A., Satomura, K., Emmons, R. V., Rowe, D. W., and Robey, P. G. (1997) *Transplantation* **63,** 1059–1069
31. Chen, X. D., Fisher, L. W., Robey, P. G., and Young, M. F. (2004) *FASEB J.* **18,** 948–958
32. Hogan, B. L. (1996) *Curr. Opin. Genet. Dev.* **6,** 432–438
33. Hoffmann, A., and Gross, G. (2001) *Crit. Rev. Eukaryot. Gene Expr.* **11,** 23–45
34. Bloom, B. B., Humphries, D. E., Kuang, P. P., Fine, A., and Goldstein, R. H. (1996) *Biochim. Biophys. Acta* **1312,** 243–248
35. Miyazono, K. (2000) *J. Cell Sci.* **113,** 1101–1109
36. Derynck, R., Zhang, Y., and Feng, X. H. (1998) *Cell* **95,** 737–740
37. Massague, J. (2000) *Nat. Rev. Mol. Cell. Biol.* **1,** 169–178
38. Yanagisawa, K., Osada, H., Masuda, A., Kondo, M., Saito, T., Yatabe, Y., Takagi, K., and Takahashi, T. (1998) *Oncogene.* **17,** 1743–1747
39. Kim, B. C., Mamura, M., Choi, K. S., Calabretta, B., and Kim, S. J. (2002) *Mol. Cell. Biol.* **22,** 1369–1378
40. Nunez, G., Benedict, M. A., Hu, Y., and Inohara, N. (1998) *Oncogene* **17,** 3237–3245
41. Bonewald, L. F., and Dallas, S. L. (1994) *J. Cell. Biochem.* **55,** 350–357
42. Harris, S. E., Bonewald, L. F., Harris, M. A., Sabatini, M., Dallas, S., Feng, J. Q., Ghosh-Choudhury, N., Wozney, J., and Mundy, G. R. (1994) *J. Bone Miner. Res.* **9,** 855–863
43. Centrella, M., Horowitz, M. C., Wozney, J. M., and McCarthy, T. L. (1994) *Endocr. Rev.* **15,** 27–39
44. Iozzo, R. V. (1994) *Matrix Biol.* **14,** 203–208
45. Andres, J. L., DeFalcis, D., Noda, M., and Massague, J. (1992) *J. Biol. Chem.* **267,** 5927–5930
46. Border, W. A., and Noble, N. A. (1995) *Nat. Med.* **1,** 1000–1001
47. Noble, N. A., Harper, J. R., and Border, W. A. (1992) *Prog. Growth Factor Res.* **4,** 369–382
48. Kolb, M., Margetts, P. J., Galt, T., Sime, P. J., Xing, Z., Schmidt, M., and Gauldie, J. (2001) *Am. J. Respir. Crit. Care Med.* **163,** 770–777
49. Comalada, M., Cardo, M., Xaus, J., Valledor, A. F., Lloberas, J., Ventura, F., and Celada, A. (2003) *J. Immunol.* **170,** 4450–4456
50. Yamaguchi, Y., Mann, D. M., and Ruoslahti, E. (1990) *Nature* **346,** 281–284
51. Markmann, A., Hausser, H., Schonherr, E., and Kresse, H. (2000) *Matrix Biol.* **19,** 631–636
52. Neptune, E. R., Frischmeyer, P. A., Arking, D. E., Myers, L., Bunton, T. E., Gayraud, B., Ramirez, F., Sakai, L. Y., and Dietz, H. C. (2003) *Nat. Genet.* **33,** 407–411
53. Schaefer, L., Macakova, K., Raslik, I., Micegova, M., Grone, H. J., Schonherr, E., Robenek, H., Echtermeyer, F. G., Grassel, S., Bruckner, P., Schaefer, R. M., Iozzo, R. V., and Kresse, H. (2002) *Am. J. Pathol.* **160,** 1181–1191
54. Dallas, S. L., Miyazono, K., Skerry, T. M., Mundy, G. R., and Bonewald, L. F. (1995) *J. Cell Biol.* **131,** 539–549
55. Erlebacher, A., and Derynck, R. (1996) *J. Cell Biol.* **132,** 195–210
56. Filvaroff, E., Erlebacher, A., Ye, J., Gitelman, S. E., Lotz, J., Heillman, M., and Derynck, R. (1999) *Development* **126,** 4267–4279
57. Massague, J., Cheifetz, S., Boyd, F. T., and Andres, J. L. (1990) *Ann. N. Y. Acad. Sci.* **593,** 59–72
58. Moses, H. L., Yang, E. Y., and Pietenpol, J. A. (1990) *Cell* **63,** 245–247
59. Schuster, N., and Krieglstein, K. (2002) *Cell Tissue Res.* **307,** 1–14
60. Moses, H. L., and Serra, R. (1996) *Curr. Opin. Genet. Dev.* **6,** 581–586
61. Leu, J. I., Crissey, M. A., and Taub, R. (2003) *J. Clin. Invest.* **111,** 129–139
62. Ghosh-Choudhury, N., Harris, M. A., Feng, J. Q., Mundy, G. R., and Harris, S. E. (1994) *Crit. Rev. Eukaryot. Gene Expr.* **4,** 345–355
63. Hagedorn, L., Floris, J., Suter, U., and Sommer, L. (2000) *Dev. Biol.* **228,** 57–72
64. Mabie, P. C., Mehler, M. F., and Kessler, J. A. (1999) *J. Neurosci.* **19,** 7077–7088
65. Raff, M. (1998) *Nature* **396,** 119–122
66. Hock, J. M., Krishnan, V., Onyia, J. E., Bidwell, J. P., Milas, J., and Stanislaus, D. (2001) *J. Bone Miner. Res.* **16,** 975–984
67. Lynch, M. P., Capparelli, C., Stein, J. L., Stein, G. S., and Lian, J. B. (1998) *J. Cell. Biochem.* **68,** 31–49